

## **Supporting Information**

### *In-situ* generation and evolution of polymer toroids by liquid crystallization-assisted seeded dispersion polymerization

Mingxin Zheng,<sup>‡a</sup> Qiquan Ye,<sup>‡a</sup> Xi Chen,<sup>b</sup> Min Zeng,<sup>a</sup> Guangjie Song,<sup>c</sup> Jun Zhang<sup>c</sup> and Jinying  
Yuan<sup>\*a†</sup>

- a. *Key Lab of Organic Optoelectronics and Molecular Engineering of Ministry of Education, Department of Chemistry, Tsinghua University, Beijing 100084, P.R.China. E-mail: yuanjy@mail.tsinghua.edu.cn*
- b. *School of materials science and engineering, Chang'an University, Xi'an 710061, P.R.China.*
- c. *CAS Key Laboratory of Engineering Plastics and CAS Research/Education Center for Excellence in Molecular Sciences, Institute of Chemistry, Chinese Academy of Sciences (CAS), Beijing 100190, P.R.China.*

<sup>‡</sup> *These authors contributed equally to this work.*

## 1. Experimental Section

### 1.1 Materials

*N,N*-dimethylaminoethyl methacrylate (DMA, 99%, TCI) and benzyl methacrylate (BzMA, 98%, TCI) were purified by passing through a basic alumina oxide column to remove the inhibitors prior to use. 2,2-Azobisisobutyronitrile (AIBN, 99%, J&K) was recrystallized in ethanol and stored at  $-20\text{ }^{\circ}\text{C}$ . 4,4'-Azobis(4-cyanopentanoic acid) (ACVA, 98%, J&K), 11-[4-(4-butylphenylazo)phenoxy]undecyl methacrylate (MAAz, 98%, TCI), Rhodamine B (RhB, pure, Acros), 2,6-Difluoroaniline (95%; Energy Chemical), 3,5-Difluorophenol (98%, Energy Chemical), 6-bromo-1-hexanol (97%, Meryer), Potassium iodide (99%, Adamas) was used as received. All the others not listed here are used as received. Phosphotungstic acid (PTA) (analytical grade, Beijing Chemical Co.) was dissolved in water for 0.5 % solution. 4-(4-cyanopentanoic acid) dithiobenzoate (CPADB) was synthesized according to the previous literature<sup>1</sup>. *N,N'*-diisopropylphenyl-1,6,7,12-tetrachloroperylene-3,4:9,10-tetra-carboxyl bisimide (PBI) was synthesized according to the previous literature<sup>2</sup>.

### 1.2 Synthesis of PDMA macro-CTA.

According to our previous report,<sup>3</sup> PDMA macro-CTA was synthesized by RAFT polymerization of DMA (180 mmol, 28.3 g) using CPADB (3.6 mmol, 1080 mg) as the RAFT agent and ACVA (0.6 mmol, 168 mg) as the initiator. The reactants were dissolved into 1,4-dioxane (60 mL) in a Schlenk flask. After nitrogen purging for 30 min, the mixture was stirred in an  $80\text{ }^{\circ}\text{C}$  oil bath for 6 h. The  $^1\text{H}$  NMR spectrum indicated that the monomer conversion reached 72%. The solution was quenched in liquid nitrogen and precipitated into n-hexane (800 mL). After drying, PDMA macro-CTA was collected. The degree of polymerization (DP) PDMA<sub>37</sub> macro-CTA was 37 ( $M_{n,\text{NMR}} = 5.3\text{ kDa}$ ) as characterized by  $^1\text{H}$  NMR measurements.

### 1.3 Preparation of PDMA<sub>37</sub>-*b*-PBzMA<sub>53</sub> assemblies by PISA.

PDMA<sub>37</sub>-*b*-PBzMA<sub>53</sub> were prepared via RAFT dispersion polymerization of BzMA in

ethanol at 15 wt % solids content. AIBN (0.05 mmol, 8.21 mg), PDMA<sub>37</sub> macro-CTA (0.2 mmol, 1.22 g) and BzMA (12.0 mmol, 2.16 g) were dissolved in ethanol (24.0 mL). The mixture was bubbled with nitrogen for 30 min, then stirred at 70 °C oil bath for 12 h. After quenching the polymerization in liquid nitrogen, the dispersion was dialyzed in alcohol to remove residual monomers for 3 days. An aliquot of the dispersion was evaporated to dryness for <sup>1</sup>H NMR and SEC characterizations, and solid content of the dispersion was measured as 109.2 mg·mL<sup>-1</sup>. The degree of polymerization (DP) of PBzMA was 53 as characterized by <sup>1</sup>H NMR.

#### **1.4 Preparation of PDMA<sub>37</sub>-*b*-PBzMA<sub>53</sub>-*b*-PMAAz<sub>*n*</sub> assemblies by seeded polymerization.**

A series of PDMA<sub>37</sub>-*b*-PBzMA<sub>53</sub>-*b*-PMAAz<sub>*n*</sub> triblock copolymer assemblies were prepared by seeded RAFT dispersion polymerization in ethanol at 5 wt % solids using the PDMA<sub>37</sub>-*b*-PBzMA<sub>53</sub> assemblies as the seeds. Taking PDMA<sub>37</sub>-*b*-PBzMA<sub>53</sub>-*b*-PMAAz<sub>54</sub> as an example, AIBN (3.29 μmol, 0.54 mg), alcoholic dispersion of PDMA<sub>37</sub>-*b*-PBzMA<sub>53</sub> (1.41 mL, containing 10 μmol of PDMA<sub>37</sub>-*b*-PBzMA<sub>53</sub> macro-CTA), and MAAz (0.60 mmol, 0.296 g) were mixed into ethanol (9.43 mL) in a Schlenk tube and bubbled with nitrogen for 30 min. The MAAz monomer was insufficiently soluble at room temperature in ethanol, but completely dissolved at 70 °C.<sup>4</sup> Then the mixture was stirred in 70 °C oil bath for 24 h. After quenching the polymerization in liquid nitrogen, the dispersion was dialyzed against ethanol to remove residual monomers. An aliquot was further purified by evaporation and vacuum-drying for NMR and SEC characterizations.

#### **1.5 Preparation of PDMA<sub>37</sub>-*b*-PBzMA<sub>137</sub> assemblies by PISA.**

PDMA<sub>37</sub>-*b*-PBzMA<sub>137</sub> were prepared via RAFT dispersion polymerization of BzMA in ethanol at 15 wt % solids content. AIBN (0.05 mmol, 8.21 mg), PDMA<sub>37</sub> macro-CTA (0.2 mmol, 1.22 g) and BzMA (30.0 mmol, 5.29 g) were dissolved in ethanol (46.8 mL). The mixture was bubbled with nitrogen for 30 min, then stirred at 70 °C oil bath

for 12 h. After quenching the polymerization in liquid nitrogen, the dispersion was dialyzed in alcohol to remove residual monomers for 3 days. An aliquot of the dispersion was evaporated to dryness for  $^1\text{H}$  NMR and SEC characterizations, and solid content of the dispersion was measured as  $104.8 \text{ mg}\cdot\text{mL}^{-1}$ .

### **1.6 Preparation of PDMA<sub>37</sub>-*b*-PBzMA<sub>137</sub>-*b*-PMAAz<sub>*n*</sub> assemblies by seeded polymerization.**

A series of PDMA<sub>37</sub>-*b*-PBzMA<sub>137</sub>-*b*-PMAAz<sub>*x*</sub> triblock copolymer assemblies were prepared by seeded RAFT dispersion polymerization in ethanol at 5 wt % solids using the PDMA<sub>37</sub>-*b*-PBzMA<sub>137</sub> assemblies as the seeds. Taking PDMA<sub>37</sub>-*b*-PBzMA<sub>137</sub>-*b*-PMAAz<sub>27</sub> as an example, AIBN (3.29  $\mu\text{mol}$ , 0.54 mg), alcoholic dispersion of PDMA<sub>37</sub>-*b*-PBzMA<sub>137</sub> (1.44 mL, containing 5  $\mu\text{mol}$  of PDMA<sub>37</sub>-*b*-PBzMA<sub>137</sub> macro-CTA), and MAAz (0.15 mmol, 0.074 g) were mixed into ethanol (3.98 mL) in a Schlenk tube. The mixture was bubbled with nitrogen for 30 min, then stirred at 70 °C oil bath for 24 h. After quenching the polymerization in liquid nitrogen, the dispersion was dialyzed against ethanol to remove residual monomers. An aliquot was further purified by evaporation and vacuum-drying for NMR and SEC characterizations.

### **1.7 Preparation of PMAAz<sub>18</sub> homopolymer.**

PMAAz homopolymer was prepared by RAFT polymerization. AIBN (6.7  $\mu\text{mol}$ , 1.87 mg), CPADB (16.7  $\mu\text{mol}$ , 4.66 mg), and MAAz (0.5 mmol, 0.2470 g) were dissolved into 4 mL of toluene and sealed in a Schlenk tube. After Ar purging for 30 min, the tube was placed into a 70 °C oil bath and polymerized for 24 h. After quenching in an ice bath, the solvent was removed under reduced pressure. The yellow powder was totally dried under high vacuum followed by the characterization.  $^1\text{H}$  NMR analysis indicated that the conversion of the polymerization was 59%, and the DP was calculated to be 18 (denoted as PMAAz<sub>18</sub>). SEC analysis showed the  $M_n$  was  $10514 \text{ g}\cdot\text{mol}^{-1}$  and PDI was 1.30.

### **1.8 Irradiation Experiments.**

The UV irradiation experiments were conducted using a CEAULIGHT CEL-M500/350 UV irradiator equipped with a high-pressure mercury lamp (500 W). The dilute dispersion of assemblies (about  $5.0 \text{ mg}\cdot\text{mL}^{-1}$ ) in a quartz bottle was placed 5–10 cm away from the lamp with stirring. The temperature of the dispersion was kept under  $35 \text{ }^\circ\text{C}$  using a water bath. A PLSSXE300/300 UV irradiator with a xenon lamp and an L-42 band-pass filter was used to generate visible light with wavelength higher than 420 nm. The UV-irradiated dispersion of assemblies (about  $5.0 \text{ mg}\cdot\text{mL}^{-1}$ ) in a quartz bottle was placed 10–15 cm away from the lamp stirring. The temperature of the sample was maintained under  $35 \text{ }^\circ\text{C}$  using a water bath.

### **1.9 Dye encapsulation of PDMA<sub>37</sub>-*b*-PBzMA<sub>137</sub> assemblies**

Hydrophilic dye was encapsulated as the preparation process of PDMA<sub>37</sub>-*b*-PBzMA<sub>137</sub> via RAFT dispersion polymerization in ethanol. AIBN (12.5  $\mu\text{mol}$ , 2.05 mg), PDMA<sub>37</sub> macro-CTA (0.05 mmol, 0.305 g), BzMA (7.5 mmol, 1.32 g) and RhB (11.7 mg) were dissolved in ethanol (11.7 mL). The mixture was bubbled with nitrogen for 30 min, then stirred at  $70 \text{ }^\circ\text{C}$  oil bath for 12 h. After quenching the polymerization in liquid nitrogen, the dispersion was dialyzed in alcohol to remove residual monomers and unencapsulated RhB for 2 days. Then, 1 mg of hydrophobic dye PBI was dissolved in 1 mL ethanol, and mixed with 1 mL RhB-encapsulated assemblies dispersion. After vigorous stirring for 12 h at room temperature, the dispersion was diluted with ethanol to 10 mL and dialyzed in alcohol to remove unencapsulated PBI for 2 days.

### **1.10 Synthesis of 2,6,2',6'-tetrafluoro-(4-hydroxy) azobenzene (FAzo)**

2,6-difluoroaniline (6.45 g, 50 mmol) were dissolved in 15 mL of concentrated hydrochloric acid, then 15 mL of water was added. The resulting solution was cooled to  $0 \text{ }^\circ\text{C}$  under stirring. Sodium nitrite (3.80 g, 55 mmol) dissolved in 50 mL cold water was added dropwise at the temperature in the range 0 to  $5 \text{ }^\circ\text{C}$ . After the solution of diazonium salt was formed, the resulting mixture was stirred for 30 min and slowly

added to 3,5-difluorophenol (6.50 g, 50 mmol) in sodium hydroxide solution (5 g, 125 mmol in 125 mL water) at 0 °C. During adding the solution of diazonium salt, the pH of the mixture solution was maintained at 9 to 10 by adding sodium carbonate (50 g, 400 mL water). The solution was vigorously stirred at 0 °C for 30 min, then stirred for 12 h at room temperature. Hydrochloric acid aqueous solution (2 mol·L<sup>-1</sup>) was added to adjust the pH to 5 to 7. The solution was kept for 10 min, and then the precipitate was filtered, washed with water and dried. Crude product was purified by column chromatography (silica gel, CH<sub>2</sub>Cl<sub>2</sub>). (7.88 g, yield: 58%). <sup>1</sup>H NMR (400 MHz, CDCl<sub>3</sub>, δ), (TMS, ppm): 6.54 (2H, ArH), 7.03 (2H, ArH), 7.31 (1H, ArH).

### **1.11 Synthesis of 2,6,2',6'-tetrafluoro-(4-(6-hydroxyhexyloxy)) azobenzene (FAzoC6)**

To 7.88 g of FAzo (29.2 mmol) in 450 mL of DMF was added 4.65 mL of 6-bromo-1-hexanol (35.3 mmol), 18.75 g of anhydrous potassium carbonate (136 mmol) and 0.5 g of potassium iodide (3.01 mmol). The resulting mixture was stirred for 24 h at 70 °C, monitored by TLC. After cooling to room temperature, the reaction mixture was poured into ice water and extracted with ethyl acetate. The organic layer was washed with 10% potassium carbonate solutions, water and saturated brine, then dried over anhydrous NaSO<sub>4</sub>. The solvent was evaporated under vacuum, and red product was further purified using column chromatography (silica gel, CH<sub>2</sub>Cl<sub>2</sub>). (7.05 g, yield: 65%). <sup>1</sup>H NMR (400 MHz, CDCl<sub>3</sub>, δ), (TMS, ppm): 1.40-1.90 (8H, C-CH<sub>2</sub>-C), 3.68 (2H, CH<sub>2</sub>OH), 4.02 (2H, ArO-CH<sub>2</sub>-C), 6.58 (2H, ArH), 7.03 (2H, ArH), 7.31 (1H, ArH).

### **1.12 Synthesis of 6-(4-((2,6-difluorophenyl) diazenyl)-3,5-difluorophenoxy) hexyl Methacrylate (MAFAz)**

FAzoC6 (7.05 g, 19 mmol) and trimethylamine (4.82 g, 48 mmol) were mixed in anhydrous CH<sub>2</sub>Cl<sub>2</sub> (100 mL) in an ice bath. A solution of 3.69 g (38 mmol) of methacryloyl chloride in anhydrous CH<sub>2</sub>Cl<sub>2</sub> (20 mL) was added dropwise over 1 h. The completion of the reaction was checked by thin layer chromatography using CH<sub>2</sub>Cl<sub>2</sub> as

eluent. Then the reaction mixture was washed with water and saturated brine. The organic phase was dried over anhydrous NaSO<sub>4</sub> and evaporated under vacuum. The orange product was further purified using column chromatography (silica gel, CH<sub>2</sub>Cl<sub>2</sub>). <sup>1</sup>H NMR (400 MHz, CDCl<sub>3</sub>, δ), (TMS, ppm): 1.40-1.90 (8H, C-CH<sub>2</sub>-C), 1.95 (3H, CH<sub>3</sub>-C=CH<sub>2</sub>), 4.02 (2H, -CH<sub>2</sub>OCO-), 4.17 (2H, ArO-CH<sub>2</sub>-C), 5.56 (1H, CH<sub>3</sub>-C=CH<sub>2</sub>), 6.11 (1H, CH<sub>3</sub>-C=CH<sub>2</sub>), 6.58 (2H, ArH), 7.03 (2H, ArH), 7.31(1H, ArH).

### 1.13 Preparation of PDMA<sub>37</sub>-*b*-PBzMA<sub>137</sub>-*b*-PMAFAz<sub>20</sub> assemblies by seeded polymerization.

PDMA<sub>37</sub>-*b*-PBzMA<sub>137</sub>-*b*-PMAFAz<sub>20</sub> triblock copolymer assemblies were prepared by seeded RAFT dispersion polymerization in ethanol at 5 wt % solids using the PDMA<sub>37</sub>-*b*-PBzMA<sub>137</sub> assemblies as the seeds. AIBN (3.29 μmol, 0.54 mg), alcoholic dispersion of PDMA<sub>37</sub>-*b*-PBzMA<sub>137</sub> (1.44 mL, containing 5 μmol of PDMA<sub>37</sub>-*b*-PBzMA<sub>137</sub> macro-CTA), and MAFAz (0.15 mmol, 0.066 g) were mixed into ethanol (3.77 mL) in a Schlenk tube. The mixture was bubbled with nitrogen for 30 min, then stirred at 70 °C oil bath for 24 h. After quenching the polymerization in liquid nitrogen, the dispersion was dialyzed against ethanol to remove residual monomers. <sup>1</sup>H NMR analysis indicated that the DP of PMAFAz was calculated to be 20 (denoted as PMAAz<sub>18</sub>). <sup>1</sup>H NMR (400 MHz, CDCl<sub>3</sub>, δ), (TMS, ppm): 4.78-5.00 (274H, Ar-CH<sub>2</sub>-O of PBzMA), 6.45-6.60 (40H, ArH of PMAFAz).

### 1.14 Post-polymerization self-assembly of PDMA<sub>37</sub>-*b*-PBzMA<sub>137</sub>-*b*-PMAAz<sub>27</sub>.

A portion of dispersion of PDMA<sub>37</sub>-*b*-PBzMA<sub>137</sub>-*b*-PMAAz<sub>27</sub> toroidal assemblies was purified by evaporation and vacuum-drying to absolutely remove ethanol. Then 0.5 mg of the copolymer was dissolved in 200 μL of CH<sub>2</sub>Cl<sub>2</sub>, and 1 mL ethanol was added to it dropwise for 20 min with constant stirring. The solution was dialyzed against ethanol to remove residual CH<sub>2</sub>Cl<sub>2</sub>.

## 2. Characterization

**2.1 <sup>1</sup>H NMR Spectroscopy:** All the <sup>1</sup>H NMR spectra were recorded on a 400 MHz JEOL JNM-ECA 400 spectrometer using CDCl<sub>3</sub> as the solvent.

**2.2 Size-Exclusion Chromatography (SEC):** All the number average molecular weights (*M<sub>n</sub>*) and polydispersity index (*D*) of the polymers were characterized by a Waters 1515 size exclusion chromatography (SEC) system at 35 °C with using THF (containing 2% trimethylamine) as the eluent at a flow rate of 1 mL/min. A series of narrow-dispersed polystyrene standards were used for SEC calibration.

**2.3 Dynamic Light Scattering (DLS):** Dynamic light scattering (DLS) measurements were carried out on a Malvern Zetasizer Nano ZS90 at 25 °C with a He-Ne laser operating at 632.8 nm. Scattering light was detected at 90° to determine intensity-average hydrodynamic diameters. The dispersions were diluted at approximately 1 mg/mL for the DLS measurements.

**2.4 Transmission Electron Microscope (TEM):** Morphologies of the samples were observed using Hitachi H-7650B transmission electron microscope (TEM) at the accelerating voltage of 80 kV. The dispersions were diluted at approximately 0.3 mg/mL. 10 μL of the diluted dispersion was dropped onto a 400-mesh carbon-coated copper grid for ambient drying. The samples were stained with phosphotungstic acid (PTA) solution (0.5 wt%) to enhance the contrast of the TEM images.

**2.5 UV Visible Spectroscopy (UV-vis):** The UV–vis spectra were recorded in ethanol by a PerkinElmer Lambda 35 spectrophotometer from 240 nm to 700 nm at a bandwidth of 1 nm. All measurements were performed using UV-grade cuvettes. The dispersions were diluted by suitable multiples for UV–vis measurement. The spectra were background corrected by subtraction of a baseline for pure ethanol.

**2.6 Atomic Force Microscope (AFM):** For each measurement, the dispersion was diluted by suitable multiples and deposited onto the freshly cleaved mica surface for absorption. After 3 h, the atomic force microscope (AFM) imaging was conducted using Scan-Asyst Fluid+probes in fluid on a Bruker Multimode 8 atomic force microscope.

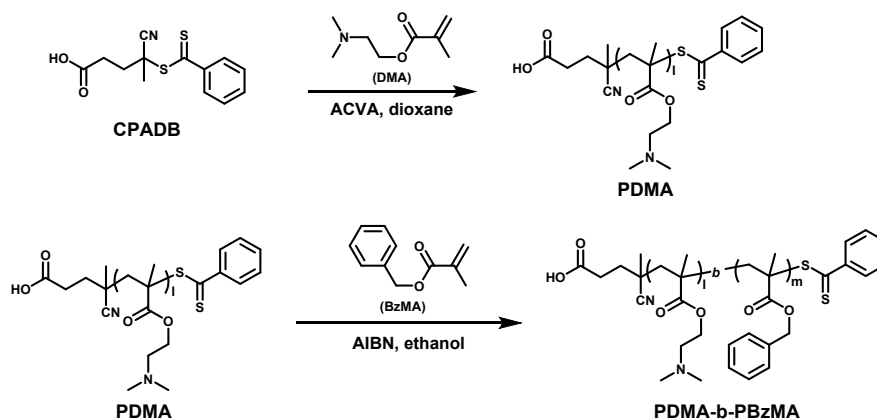


**2.7 Small Angle X-ray Scattering (SAXS):** Small angle X-ray scattering (SAXS) of the colloidal solution was performed on a Xenocs Xeuss 2.0 instrument with a Cu K $\alpha$  radiation source ( $\lambda = 0.154$  nm) operating at approximately 8 keV and a Pilatus 200 K-A detector with a sample-to-detector distance of about 1 m. 1-D integrated data were obtained averaging over  $0.11 \leq q$  (nm $^{-1}$ )  $\leq 4.70$  and  $0 \leq x \leq 360$ . The exposure time was 1 h for dispersion samples and 20 min for solid samples, respectively. The scattering intensity was corrected for background and mask.

**2.8 Differential Scanning Calorimeter (DSC):** The sample from seeded polymerization was volatilized for 48 h in room temperature to remove ethanol. DSC analyses were measured with a Q2000 (TA Instruments, USA). The measure procedure consists of two scanning cycles under N $_2$  flow from 20 °C to 150 °C, where both the heating and cooling rates were 10 °C min $^{-1}$ , and the first scanning was in order to eliminate the thermal history of the sample.

**2.9 Confocal Laser Scanning Microscopy (CLSM):** The morphology of the fluorescent dye-encapsulated assemblies was characterized *in situ* by a confocal laser scanning microscope (LSM 710, Carl Zeiss, Germany) with a 25 $\times$  water-immersion objective. Image processing was achieved with the Image viewer (Carl Zeiss, Germany). PBI was excited at 488 nm and recorded between 500 and 540 nm. RhB was excited at 552 nm and recorded between 565 and 590 nm.

### 3. Molecular characterization of polymer



Scheme S1. Synthetic route to the PDMA-*b*-PBzMA diblock copolymers.

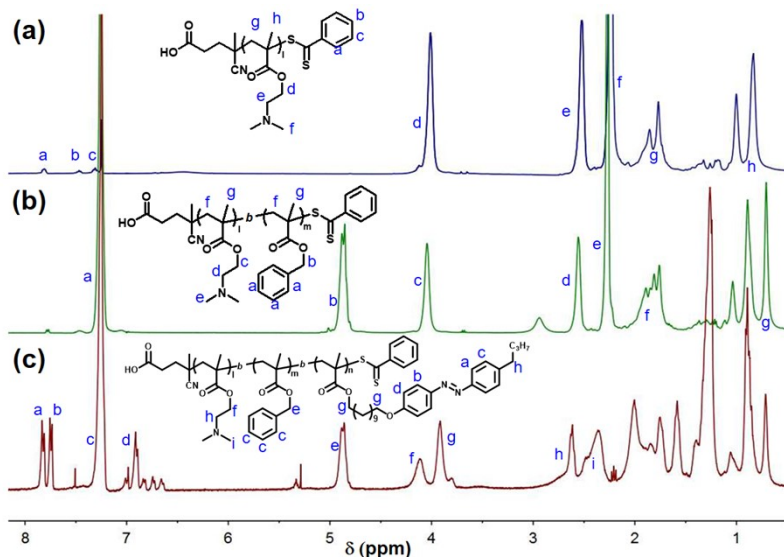
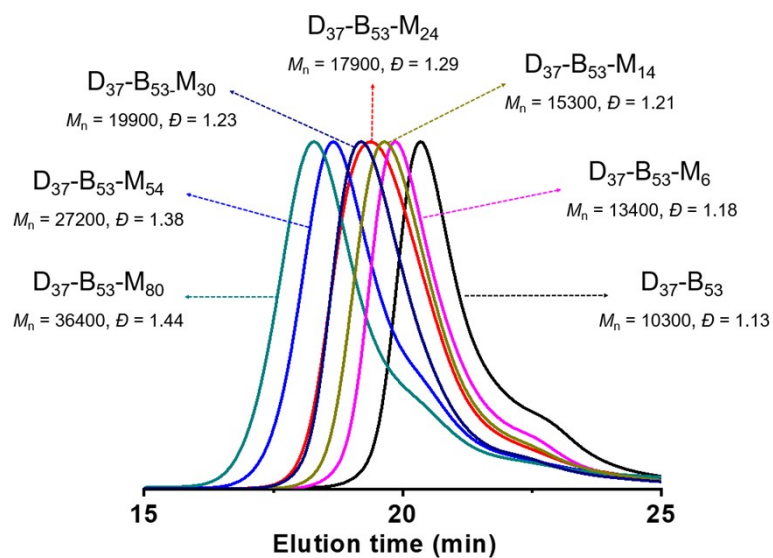


Figure S1. <sup>1</sup>H NMR spectra (solvent: CDCl<sub>3</sub>) of (a) PDMA<sub>37</sub>; (b) PDMA<sub>37</sub>-*b*-PBzMA<sub>53</sub> and (c) PDMA<sub>37</sub>-*b*-PBzMA<sub>53</sub>-*b*-PMAAz<sub>24</sub>. DPs of PDMA macro-CTA, PBzMA and PMAAz were calculated via comparing the integral area ( $I_i$ ) ratio of peak, as

$$(a) DP_{PDMA} = \frac{5I_d}{2(I_a + I_b + I_c)}$$

$$(b) DP_{PBzMA} = \frac{I_b}{I_c} \cdot DP_{PDMA}$$

$$(c) DP_{PMAAz} = \frac{I_a + I_b}{2I_f} \cdot DP_{PDMA}$$



**Figure S2.** SEC traces of PDMA<sub>37</sub>-*b*-PBzMA<sub>53</sub> and PDMA<sub>37</sub>-*b*-PBzMA<sub>53</sub>-*b*-PMAAz<sub>*n*</sub> (D<sub>37</sub>-B<sub>53</sub>-M<sub>*n*</sub>) copolymers (THF, polystyrene standards).

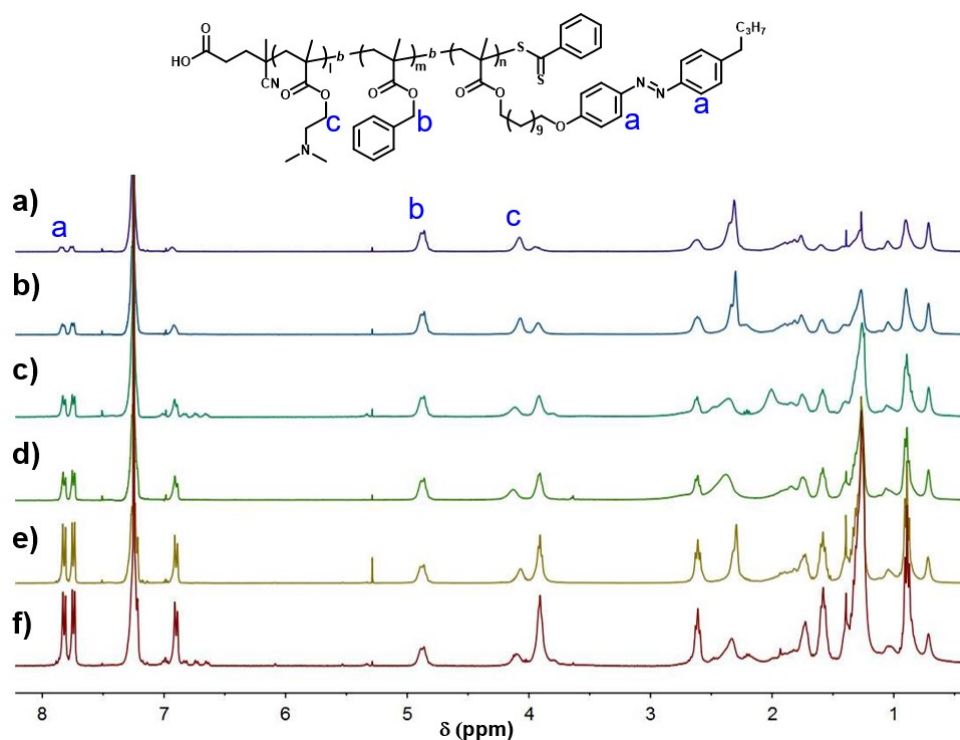


**Figure S3.** <sup>1</sup>H NMR spectra of PDMA<sub>37</sub>-*b*-PBzMA<sub>53</sub> and PDMA<sub>37</sub>-*b*-PBzMA<sub>53</sub>-*b*-PMAAz<sub>*n*</sub> copolymers, *n* = a) 6, b) 14, c) 24, d) 30, e) 54 f) 80. (solvent: CDCl<sub>3</sub>).

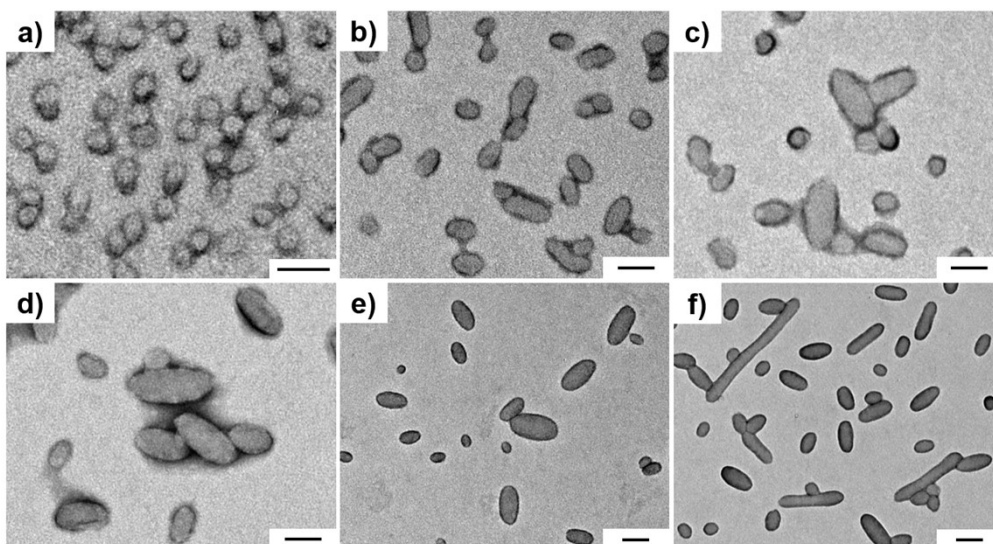


**Figure S4.** TEM images of a)  $\text{PDMA}_{37}\text{-}b\text{-PBzMA}_{53}$ , and  $\text{PDMA}_{37}\text{-}b\text{-PBzMA}_{53}\text{-}b\text{-PMAAz}_n$  copolymer assemblies,  $n =$  b) 6, c) 14, d) 24, e) 30, f) 54. Scale bars: 50 nm in a–d), 100 nm in e) and f).

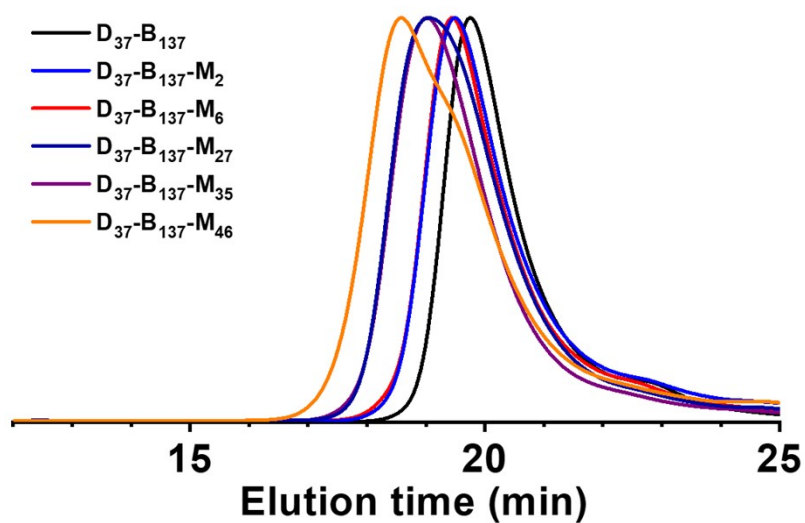


**Figure S5.** SEC traces of  $\text{PDMA}_{37}\text{-}b\text{-PBzMA}_{137}$  and  $\text{PDMA}_{37}\text{-}b\text{-PBzMA}_{137}\text{-}b\text{-PMAAz}_n$  ( $\text{D}_{37}\text{-B}_{137}\text{-M}_n$ ) copolymers (THF, polystyrene standards).

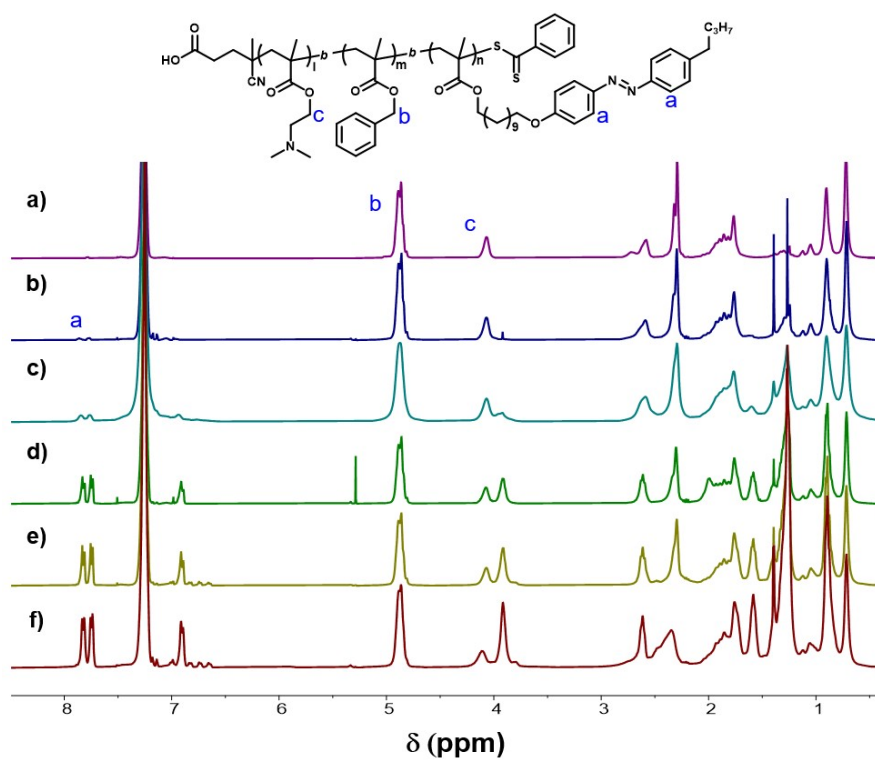


**Figure S6.** <sup>1</sup>H NMR spectra of PDMA<sub>37</sub>-b-PBzMA<sub>137</sub> and PDMA<sub>37</sub>-b-PBzMA<sub>137</sub>-b-PMAAz<sub>n</sub> copolymers,  $n = (a) 0, (b) 2, (c) 6, (d) 27, (e) 35, (f) 46$  (solvent: CDCl<sub>3</sub>).

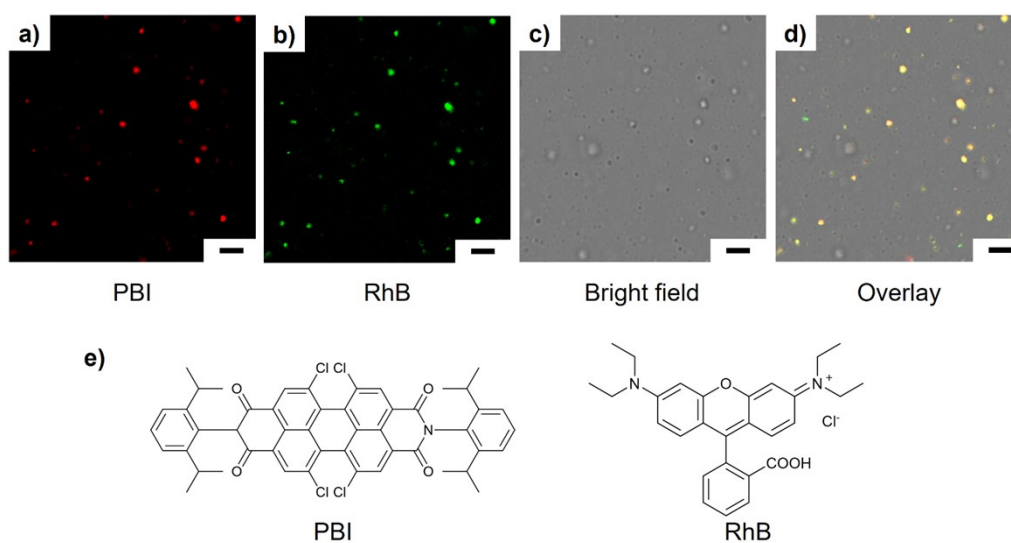


**Figure S7.** CLSM images of PBI- and RhB-loaded PDMA<sub>37</sub>-*b*-PMAAZ<sub>137</sub> vesicles. a) PBI, b) RhB, c) bright field, d) overlay. e) Chemical structure of hydrophobic PBI and hydrophilic RhB. Scale bars: 5  $\mu$ m in a-d).

To identify the vesicular structure of PDMA<sub>37</sub>-*b*-PMAAZ<sub>137</sub> seeds. We examined whether the membrane could encapsulate hydrophobic molecules (Fig. S7a) by incorporating hydrophobic PBI stain within it. Although the resolution of the fluorescence optical microscope could not allow precise location to be determined, the light-emitting spherical particles confirmed the dye's presence in vesicles. Vesicular assemblies could also accommodate hydrophilic molecules, such as RhB. After encapsulation, the fluorescence of particles was evaluated to confirm the presence of RhB in the lumen (Fig. S7b). These studies further indicated the vesicular construct of PDMA<sub>37</sub>-*b*-PMAAZ<sub>137</sub> seeds, which is corresponding with the TEM image.

**Table S1.** Feed ratio, DP of PMAAZ, monomer conversion, molecular weight, polydispersity and final morphology obtained from a series of PDMA-*b*-PBzMA-*b*-PMAAZ (D-B-M) triblock copolymers.

Sample	Feed <sup>a</sup>	DP <sub>PMAAZ</sub> <sup>c</sup>	Conv. <sup>d</sup> (%)	$M_n$ <sup>e</sup> (kDa)	$\bar{D}$ <sup>e</sup>	Morphology <sup>g</sup>
D <sub>37</sub> -B <sub>53</sub>	–	–	–	10.3	1.13	sphere
D <sub>37</sub> -B <sub>53</sub> -M <sub>6</sub>	10	6	60	13.4	1.18	ellipsoid
D <sub>37</sub> -B <sub>53</sub> -M <sub>14</sub>	20	14	70	15.3	1.21	ellipsoid
D <sub>37</sub> -B <sub>53</sub> -M <sub>24</sub>	30	24	80	17.9	1.29	ellipsoid
D <sub>37</sub> -B <sub>53</sub> -M <sub>30</sub>	40	30	75	19.9	1.23	ellipsoid
D <sub>37</sub> -B <sub>53</sub> -M <sub>54</sub>	60	54	90	27.2	1.38	cylinder
D <sub>37</sub> -B <sub>53</sub> -M <sub>80</sub>	120	80	67	36.4	1.44	cylinder
D <sub>37</sub> -B <sub>137</sub>	–	–	–	14.3	1.16	vesicle
D <sub>37</sub> -B <sub>137</sub> -M <sub>2</sub>	5	2	40	16.3	1.22	“tadpole”
D <sub>37</sub> -B <sub>137</sub> -M <sub>6</sub>	10	6	60	16.7	1.22	“clover”
D <sub>37</sub> -B <sub>137</sub> -M <sub>27</sub>	30	27	90	22.5	1.26	toroid
D <sub>37</sub> -B <sub>137</sub> -M <sub>35</sub>	40	35	88	22.5	1.23	cylinder
D <sub>37</sub> -B <sub>137</sub> -M <sub>46</sub>	50	46	92	25.1	1.42	cylinder

<sup>b</sup>The feed molar ratio of the MAAz monomer to D<sub>37</sub>-B<sub>x</sub> macro-CTA.

<sup>c</sup>Determined by <sup>1</sup>H NMR spectroscopy in CDCl<sub>3</sub>.

<sup>d</sup>Calculated according to <sup>1</sup>H NMR data.

<sup>e</sup>Determined by SEC in THF;  $\bar{D} = M_w / M_n$ .

<sup>g</sup>Determined by TEM observations.

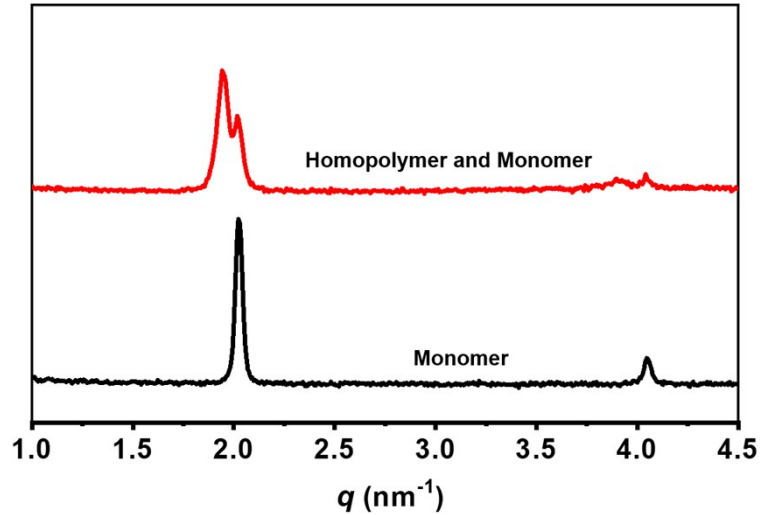


**Figure S8.** SAXS pattern of the MAAz monomer and a mixture of PMAAZ<sub>18</sub> homopolymer and MAAz monomer.

To identify the LC ordered nanostructure, MAAz monomer and PMAAZ homopolymer were characterized by SAXS. Compared with low concentration of dispersion, solid samples showed stronger signal peaks without influence of solvent scattering. The scattering peak was located at 2.03 nm<sup>-1</sup> and the second order scattering peak was also observed at 4.06 nm<sup>-1</sup> for MAAz. The pattern of a mixture of PMAAZ<sub>18</sub> and MAAz showed that the peak position of homopolymer was just slightly different from monomer. The results indicated that assemblies have similar LC-microphase with MAAz monomer and its homopolymer.

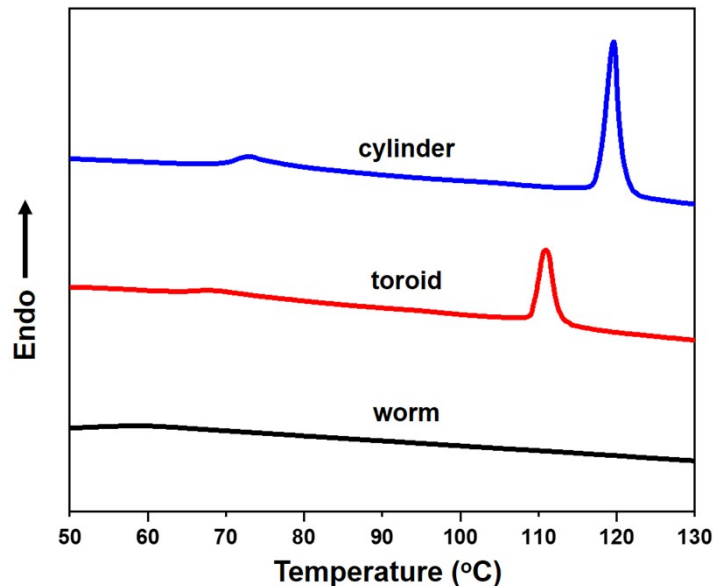


**Figure S9.** DSC curves of the PDMA<sub>37</sub>-*b*-PBzMA<sub>53</sub>-*b*-PMAAZ<sub>54</sub> cylinder, PDMA<sub>37</sub>-*b*-PBzMA<sub>137</sub>-*b*-PMAAZ<sub>27</sub> toroid and PDMA<sub>37</sub>-*b*-PBzMA<sub>137</sub>-*b*-PMAAZ<sub>2</sub> worm on the heating process.



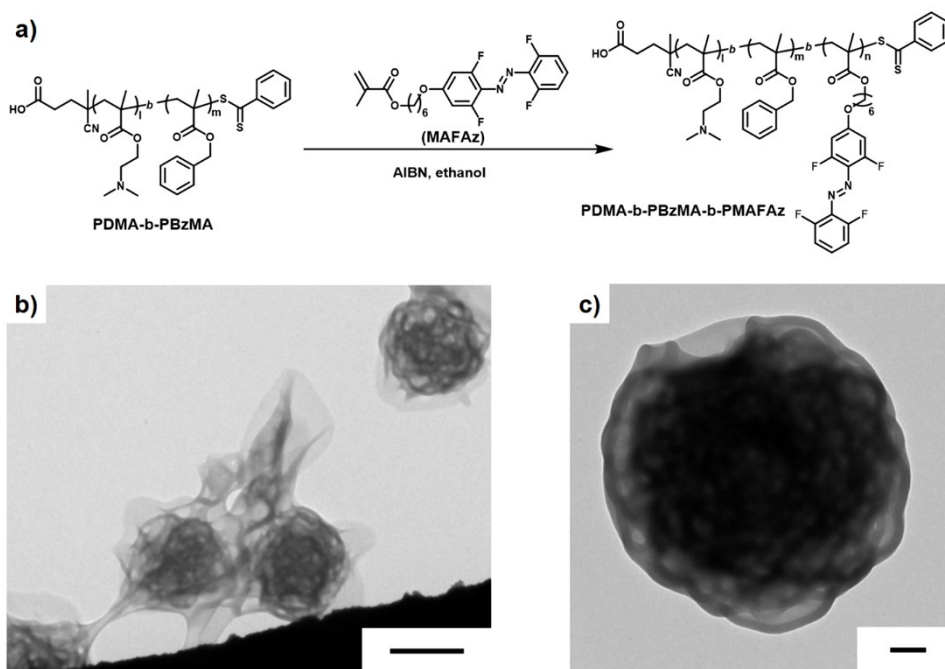


**Figure S10.** a) Preparation of PDMA-*b*-PBzMA-*b*-PMAFAz triblock copolymers *via* seeded dispersion polymerization; b) TEM image of PDMA<sub>37</sub>-*b*-PBzMA<sub>137</sub>-*b*-PMAFAz<sub>20</sub> assemblies. Scale bar: 1  $\mu\text{m}$  and 200 nm in b) and c).

To further confirm that LC property of azobenzene copolymer is necessary for the formation of toroids, we synthesized another azobenzene monomer MAFAz which has intermolecular  $\pi$ - $\pi$  stacking and comparable size with MAAz but without LC property according to the literature.<sup>5</sup> We conducted a control experiment under the same conditions of polymerization of toroidal assemblies, and PDMA<sub>37</sub>-*b*-PBzMA<sub>137</sub>-*b*-PMAFAz<sub>20</sub> assemblies were obtained (Figure S10a). TEM image showed that large compound vesicles (LCVs) or sponge-like particles were obtained with ill-defined bicontinuous structures and a size of about 1.5  $\mu\text{m}$ . This is similar to a kind of classical feature of PISA that increasing solvophobic block length leads to a sequential morphological evolution from vesicles to LCVs to sponge-like particles and finally to inverse bicontinuous structures.<sup>6</sup> Therefore, the formation of toroids was assisted by both LC interaction and hydrophilic-hydrophobic balance.

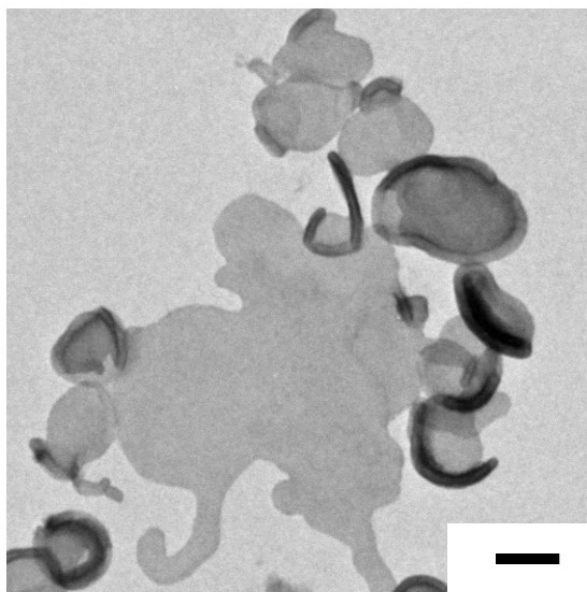


**Figure S11.** TEM image of post-polymerization self-assembly of PDMA<sub>37</sub>-*b*-PBzMA<sub>137</sub>-*b*-PMAAZ<sub>27</sub>.

In seeded polymerization formulation, self-assembly during polymerization *in situ* may lead to different morphologies compared with post-polymerization self-assembly. We conduct a control experiment with the same copolymer of PDMA<sub>37</sub>-*b*-PBzMA<sub>137</sub>-*b*-PMAAZ<sub>27</sub> toroids through a process of drying and redissolution. As ethanol was added dropwise into dichloromethane solution of copolymer, self-assemblies were regenerated. TEM image showed that lamella was a typical morphology in absence of seeded polymerization. Therefore, the formation of toroids is associated with *in-situ* polymerization method in this study.

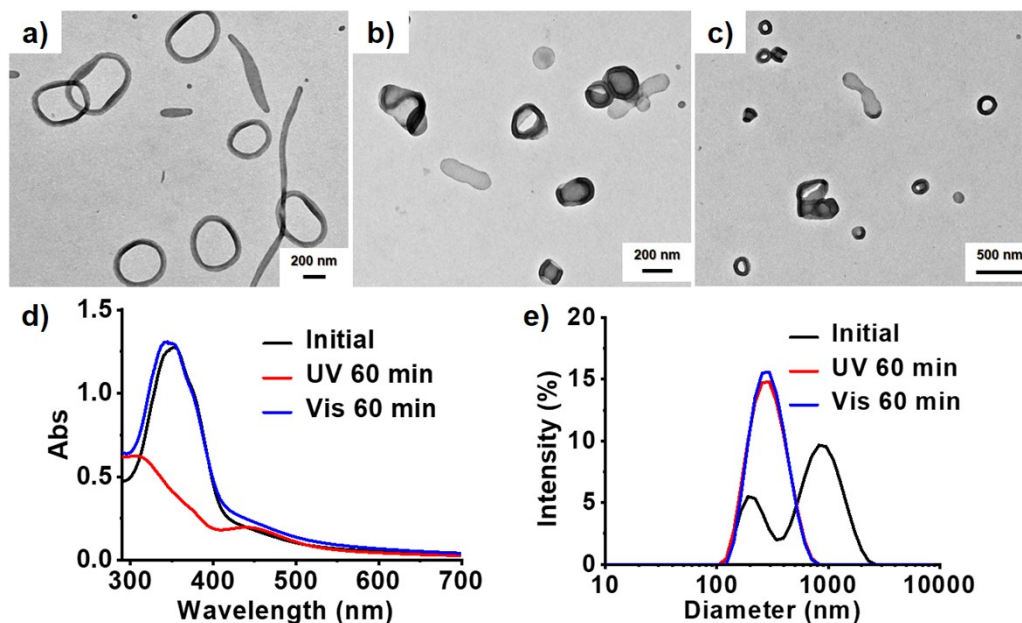


**Figure S11.** TEM images of PDMA<sub>37</sub>-*b*-PBzMA<sub>137</sub>-*b*-PMAAZ<sub>27</sub> assemblies a) before and b) after UV irradiation for 60 min. c) TEM images of the UV-irradiated assemblies after visible light irradiation for 60 min. d) UV-vis spectra and e) DLS measurements of PDMA<sub>37</sub>-*b*-PBzMA<sub>137</sub>-*b*-PMAAZ<sub>27</sub> assemblies before and after UV irradiation for 60 min, and the UV-irradiated assemblies after visible light irradiation for 60 min.

To evaluate the reversibility of the phototriggered morphology transformation, assembly dispersion of PDMA<sub>37</sub>-*b*-PBzMA<sub>137</sub>-*b*-PMAAZ<sub>27</sub> after UV irradiation for 1 h was exposed to visible light. Initial sample manifests an absorbance maximum at 354 nm, corresponding to the  $\pi$ - $\pi^*$  transition of the *trans*-azobenzene. After UV irradiation for 1 h, the absorbance at 354 nm decreased, while the absorbance at 440 nm increased, corresponding to the  $n$ - $\pi^*$  transition of *cis*-azobenzene. Barrels are displayed in magnified TEM images with about 200 nm diameter, which is formed by the bending and fusion of lamellae (Figure S11b). Dynamic light scattering (DLS) results showed that the particle size and polydispersity of the assemblies decreased significantly after UV irradiation for 1 h, and the final particle size was 200–300 nm, which was consistent with the particle size of the lamellar and cylindrical assemblies observed by TEM. After visible light irradiation for 1 h, the absorbance at 354 nm increased, which corresponded to the initial absorbance value before UV irradiation, indicating *cis*-to-*trans* isomerization of azobenzene groups (Figure S11d). But TEM shows still lamellae and

barrels (Figure S11c), and DLS result is no obvious change (Figure S11e). Due to the limited number of azobenzene groups in PDMA<sub>37</sub>-*b*-PBzMA<sub>137</sub>-*b*-PMAAZ<sub>27</sub>, it is not enough to cause reversed transformation of kinetically trapped copolymer morphologies upon visible light irradiation.

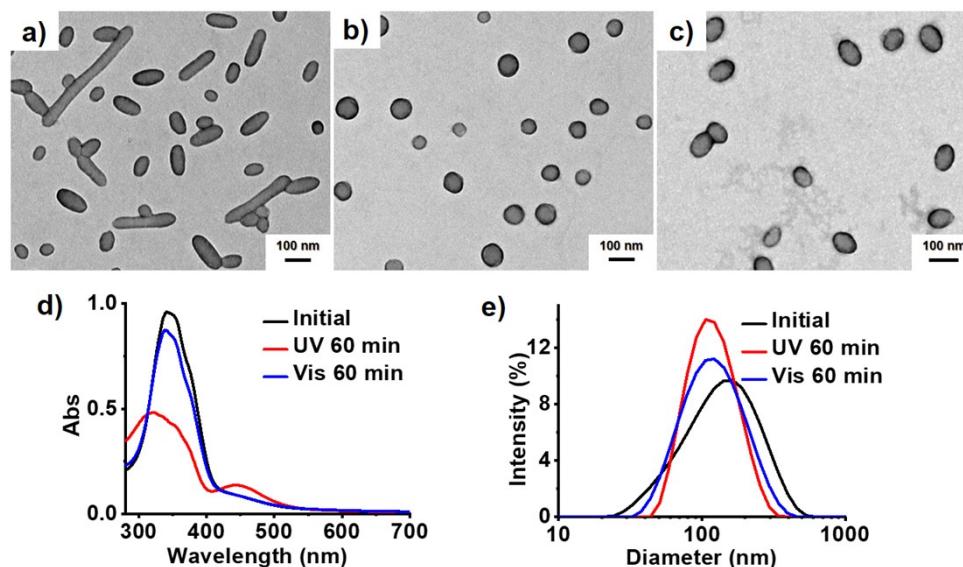


**Figure S12.** TEM images of PDMA<sub>37</sub>-*b*-PBzMA<sub>53</sub>-*b*-PMAAZ<sub>54</sub> assemblies a) before and b) after UV irradiation for 60 min. c) TEM images of the UV-irradiated assemblies after visible light irradiation for 60 min. d) UV-vis spectra and e) DLS measurements of PDMA<sub>37</sub>-*b*-PBzMA<sub>53</sub>-*b*-PMAAZ<sub>54</sub> assemblies before and after UV irradiation for 60 min, and the UV-irradiated assemblies after visible light irradiation for 60 min.

Cylindrical micelles of PDMA<sub>37</sub>-*b*-PBzMA<sub>53</sub>-*b*-PMAAZ<sub>54</sub> were also irradiated with UV and visible light, and characterized the morphological transition by TEM, UV-vis spectrum and DLS. TEM images showed that the cylinder transformed into a spherical micelle with a particle size of 60-100 nm after UV irradiation for 1 h (Figure S12b), then the assemblies transformed from spheres to ellipsoids after visible light irradiation for 1 h (Figure S12c). UV-vis absorption spectra are similar to toroidal micelles, in which the absorption peak at 365 nm decreased under the UV light and recovered after visible light irradiation (Figure S12d). DLS results showed that the particle size distribution of assemblies became significantly narrower after UV irradiation with diameter of 100 nm, while the distribution became slightly wider after visible light

irradiation (Figure S12e). This is consistent with TEM results that the size distribution of the ellipsoidal micelles is between cylinders and spheres.

The morphological transformation mechanism of cylindrical micelles is similar to that of toroids. After UV irradiation, the *trans*-azobenzene is transformed into *cis*-azobenzene, resulting in the LC-to-isotropic phase transition in the cores. The isotropic spherical micelles are formed to reduce the surface energy of the system. After visible light irradiation, the *cis*-azobenzene was converted back to *trans*. Although the assemblies cannot fuse into cylinders due to the trapping of a "kinetically frozen" state, spherical micelles are transformed into ellipsoids.

## References

1. Y. Mitsukami, M. S. Donovan, A. B. Lowe and C. L. McCormick, *Macromolecules*, 2001, **34**, 2248-2256.
2. H. Qian, C. Liu, Z. Wang and D. Zhu, *Chem. Commun.*, 2006, 4587-4589.
3. Q. Ye, M. Huo, M. Zeng, L. Liu, L. Peng, X. Wang and J. Yuan, *Macromolecules*, 2018, **51**, 3308-3314.
4. S. Guan, C. Zhang, W. Wen, T. Qu, X. Zheng, Y. Zhao and A. Chen, *ACS Macro Lett.*, 2018, **7**, 358-363.
5. L. Li, S. Cui, A. Hu, W. Zhang, Y. Li, N. Zhou, Z. Zhang and X. Zhu, *Chem. Commun.*, 2020, **56**, 6237-6240.
6. F. Lv, Z. An and P. Wu, *Nat. Commun.*, 2019, **10**, 1397.